The EcoRI−DNA Complex as a Model for Investigating Protein−DNA Interactions by Atomic Force Microscopy

Isabelle Sorel,[‡] Olivier Piétrement,*[,§] Loïc Hamon,[‡] Sonia Baconnais,[§] Eric Le Cam,[§] and David Pastré[‡]

Laboratoire Structures et Reconnaissance des Biomolécules, EA 3637, Université d'Evry, Rue du Père Jarlan, 91025 Evry Cedex, France, and Laboratoire de Microscopie Moléculaire et Cellulaire, UMR 8126 CNRS-IGR-UPS, Institut Gustave-Roussy, 39 rue Camille Desmoulins, 94805 Villejuif Cedex, France

Received February 10, 2006; Revised Manuscript Received September 13, 2006

ABSTRACT: Atomic force microscopy (AFM) is a technique widely used to image protein−DNA complexes, and its application has now been extended to the measurements of protein−DNA binding constants and specificities. However, the spreading of the protein−DNA complexes on a flat substrate, generally mica, is required prior to AFM imaging. The influence of the surface on protein−DNA interactions is therefore an issue which needs to be addressed. For that purpose, the extensively studied EcoRI−DNA complex was investigated with the aim of providing quantitative information about the surface influence. The equilibrium binding constant of the complex was determined by AFM at both low and high ionic strengths and compared to electrophoretic mobility shift assay measurements (EMSA). In addition, the effect of the DNA length on dissociation of the protein from its specific site was analyzed. It turned out that the AFM measurements are similar to those obtained by EMSA at high ionic strengths. We then advance the idea that this effect is due to the high counterion concentration near the highly negatively charged mica surface. In addition, a dissociation of the complexes once they are adsorbed onto the surface was observed, which is weakly dependent on the ionic strength contrary to what occurs in solution. Finally, a two-step mechanism, which describes the adsorption of the EcoRI−DNA complexes on the surface, is proposed. This model could also be extended to other protein−DNA complexes.

Site-specific protein−DNA interactions are fundamentally important in many biological processes like DNA reparation because they are generally the first step before the recruitment of other proteins (*1*, *2*). Many methods, such as electrophoretic mobility shift assays (EMSA)[1] or filter binding assays, are powerful techniques for investigating specific protein−DNA interactions. However, for a few years, atomic force microscopy (AFM) has also been used to study specific protein−DNA complexes at the single-molecule level (*3*, *4*). The advantage of AFM over conventional techniques is that it allows a direct visualization of the protein−DNA complex on a nanometer scale (*5*−*11*). The use of AFM in liquids also allows the imaging of ligand−DNA interactions under physiological conditions, rendering possible the real-time observation of formation of the complex, dissociation, and DNA conformational changes upon protein binding. It is also worth noting that AFM overcomes the limitation of electron microscopy (EM), which cannot be used to image small proteins like EcoRI.

Despite the AFM success among biologists, it is surprising that a quantitative study of how the substrate may influence protein−DNA interactions has not been tackled. Indeed, DNA molecules are generally adsorbed to a charged surface prior to imaging, which should change the ionic surrounding of the molecules and, therefore, the thermodynamic and kinetic constants of the protein−DNA complex. Some parameters, like the binding constant and the dissociation constant, are particularly useful in determining the protein concentration required for AFM imaging and the complex lifetime on the surface. In this article, we focus our attention on the mica surface, which is the most widely used substrate for protein−DNA complexes imaging due to its ultraflat surface. The natural repulsion between the negatively charged DNA phosphate backbone and the negatively charged mica surface is generally overcome by the addition of divalent cations (*12*, *13*) or trivalent cations (*14*) in the deposition buffer. We have previously studied the effect of the mica surface on drug−DNA interactions (*15*, *16*), and we wanted to extend our investigations to specific protein−DNA complexes. Our aim was to provide useful quantitative data about the influence of a charged surface on protein−DNA interactions. The protein that we have chosen for this investigation is EcoRI, one of the most studied restriction endonucleases. Indeed, thermodynamic parameters governing the interactions of EcoRI with DNA have been determined (*17*) as well as the structure of the EcoRI−DNA complex (*18*) and the kinetic mechanisms of association and dissociation (*19*). EcoRI is a small restriction enzyme (31 kDa), which interacts with DNA as a dimer and introduces double-strand breaks into the 5′-GAATTC-3′ sequence. In addition, the EcoRI−DNA complex has already been observed by AFM in identifying specific nucleotide sequences in plasmid

* To whom correspondence should be addressed. Telephone: (33) 1 42 11 48 79. Fax: (33) 1 42 11 54 94. E-mail: olivier.pietrement@igr.fr.

[‡] Université d'Evry.

[§] UMR 8126 CNRS-IGR-UPS.

[1] Abbreviations: AFM, atomic force microscope; EMSA, electrophoretic mobility shift assay; EM, electron microscopy.

10.1021/bi060293u CCC: $33.50
Published on Web 11/14/2006

DNA molecules (*5*). Here, the EcoRI−DNA complex was considered as a suitable model for studying the influence of the mica surface on DNA−protein interactions.

In this study, we first measured ν, the ratio of the concentration of EcoRI−DNA complexes to the total concentration of DNA molecules, by gel shift assays. Then ν was measured on the mica surface by AFM so the differences between surface measurements (AFM) and bulk measurements (EMSA) could be studied. These experiments were performed both at low and high ionic strengths. Indeed, for a highly charged surface like mica, the surface ion concentration is nearly independent of bulk ion concentration (*20*), which could influence EcoRI−DNA interactions. In a second part, we studied the effect of DNA fragment length on the AFM measurement of ν. In solution, it is generally accepted that the probability of complex dissociation is larger for the longer DNA fragment due to the nonspecific DNA binding at low and moderate ionic strengths (*21*). We checked if AFM experiments lead to the same conclusions since the surface may influence the nonspecific EcoRI−DNA interactions. Then we measured the dissociation time of the EcoRI−DNA complex once fully adsorbed on the surface, which is a crucial parameter for AFM users.

Finally, from our results, we propose a new model which describes a two-step mechanism for the complex adsorption on the surface. Some practical interests concerning the observation of protein−DNA interactions by AFM are then considered.

MATERIALS AND METHODS

DNA Fragments. The 1188 bp fragments were obtained from plasmid pBR322 by PCR amplification with the following primers: 5′-CATAGCAGAACTTTAAAAGTACTCATC-3′ (forward) and 5′-AGTTGCATGATAAAGAAGACAGTC-3′ (reverse). The PCR product was purified on an anion exchange miniQ column (Amersham Biosciences) with a SMART system (Amersham Biosciences), precipitated with ethanol, and suspended in TE buffer [10 mM Tris (pH 7.5) and 1 mM EDTA].

The 500 bp DNA fragments were produced by digesting plasmid pUC19 with restriction enzymes NdeI and SapI, isolated and purified with a miniQ column, desalted, and concentrated with a Microcon YM-100 device (Millipore) in TE buffer.

For longer fragments, pBR322 plasmids were linearized with restriction enzyme PvuII and purified by gel filtration on a Superose 6 PC 3.2/30 micro-column (Amersham Biosciences) with a SMART system.

For the construction of the 749 bp circular fragments, 959 bp fragments were obtained from PCR amplification with the following primers: 5′-ACTCTCAAGGATCCTACCGCTGTTG-3′ (forward) for which the target sequence of BamHI (5′-GGATCC-3′) is inserted and 5′-CGCAAGGAATGGTGCATGCA-3′ (reverse). The PCR product was then purified on a miniQ column, desalted, and concentrated with a Microcon YM-100 device (Millipore) in TE buffer. The 959 bp fragments were cut with restriction enzyme BamHI to produce 9, 749, and 201 bp fragments. The 749 bp fragments were isolated and purified on a miniQ column. To obtain 749 bp circle DNA molecules, 749 bp fragments were incubated at a concentration of 0.22 μg/mL in ligase buffer [50 mM Tris-HCl (pH 7.5), 10 mM $MgCl_2$, 10 mM dithiothreitol, 1 mM ATP, and 25 μg/mL bovine serum albumin] in the presence of 1 unit/μL T4 DNA ligase (New England Biolabs) for 16 h at 16 °C. The 749 bp circular DNA fragments were purified on a miniQ column, precipitated with ethanol, and suspended in TE buffer.

For each fragment, the homogeneity in DNA length was controlled with gel electrophoresis and by EM, and the concentration was quantified at 260 nm in a Genequant microspectrophotometer (Amersham Biosciences).

Enzymes. Enzymes were purchased from Sigma (EcoRI), Promega (BamHI), and New England Biolabs (NdeI and SapI) and were used without further purification. To determine the molar concentration of actively binding protein, we performed a gel mobility shift assay (see below for the protocol).

AFM Imaging. Imaging was performed in tapping mode with a multimode AFM instrument (Veeco) operating with a Nanoscope IIIa controller. We used AC160TS silicon cantilevers (Olympus) with resonance frequencies of ∼300 kHz. The applied force was minimized as much as possible. All images were collected at the scan frequency of 1.5 Hz and a resolution of 512 × 512 pixels.

For the determination of ν, only DNA molecules for which the contour length was easily distinguished were taken into account. The statistical study was carried out by analyzing ∼200 molecules for each sample.

Measurement of ν, the Ratio of the Concentration of EcoRI−DNA Complexes to the Total Concentration of Adsorbed DNA Molecules, versus EcoRI Concentration. The specific EcoRI−DNA complex was formed by incubating a 10 μL solution of the 1188 bp DNA fragment at 0.2 nM either in 20 mM NaCl and 20 mM Tris (pH 7.6) (low ionic strength) or in 300 mM NaCl and 20 mM Tris (pH 7.6) (high ionic strength) with the EcoRI protein at a concentration varying from 4 to 125 nM for 5 min at 37 °C. Then, 10 μL of a buffer containing the appropriate concentration of Ca^{2+} to ensure DNA adsorption on the surface was added to the solution. After dilution, the deposition buffer at low ionic strength consisted of 10 mM $CaCl_2$, 20 mM NaCl, and 20 mM Tris (pH 7.6). At high ionic strength, the buffer consisted of 100 mM $CaCl_2$, 300 mM NaCl, and 20 mM Tris (pH 7.6). A 5 μL droplet was deposited onto mica for 30 s. The low DNA concentration and the short deposition time limit the number of molecules adsorbed on the surface to approximately five molecules per square micrometer. Then the surface was rinsed by being plunged into a 0.02% (w/v) aqueous uranyl acetate solution to maintain the DNA molecules in their conformations (*22*) and dried with filter paper.

Dissociation of the Adsorbed EcoRI−DNA Complex versus Deposition Time. The solutions were prepared following the same protocol as the previous one with a DNA concentration of 0.2 nM and an EcoRI concentration of 60 nM, but the 5 μL droplet was deposited onto mica for 15 s. Then the drop was diluted with 45 μL of a buffer containing either 10 mM $CaCl_2$ or 100 mM $CaCl_2$ to prevent adsorption of additional DNA molecules on the surface, and the incubation time on the surface was increased from 0 to 105 s. Then the surface was rinsed and dried as described above.

AFM Imaging of a Purified Complex. The specific EcoRI−DNA complex was formed by incubating a 100 μL solution

of the 1188 bp DNA fragment at 1 nM in 20 mM Tris (pH 7.6) and 20 mM NaCl with the protein EcoRI at a concentration of 12.5 nM for 5 min at 37 °C. Then the solution was loaded onto a Superose 6 PC 3.2/30 micro-column (Amersham Biosciences), and the complex was eluted in 20 mM Tris (pH 7.6) and 20 mM NaCl in less than 2 min which is short enough to avoid its dissociation (*21*). The purified complex was immediately deposited onto mica and imaged by AFM.

EMSA Experiments. pBR322 plasmid (100 nM) was diluted in 2× reaction buffer [100 mM Tris-HCl (pH 7.5), 20 mM $MgCl_2$, 200 mM NaCl, and 2 mM dithioerythreitol]. Various concentrations of EcoRI (Sigma) were incubated for 15 min at 37 °C with 1188 bp DNA fragment (10 nM) in 10 mM Tris (pH 7.6) and 20 or 300 mM NaCl. Then cleavage reaction was initiated by mixing 5 μL of the EcoRI−DNA solution with 5 μL of pBR322−EcoRI buffer (pBR322 was added to yield a 10-fold excess over 1188 bp fragments) for 30 s, and the reaction was terminated by addition of 3 μL of 100 mM EDTA. Samples were loaded onto 1% agarose gels in 1× TBE buffer [89 mM Tris (pH 8.3), 89 mM boric acid, and 2 mM EDTA]. The gels were run at 10 V/cm and 4 °C, and DNA was stained in 1:10000 SYBR Green I (Molecular Probes) for 30 min. Gels were scanned using a Fuji FLA-3000 PhosphorScreen, and the bands were quantified using ImageGauge. ν was determined as the ratio between two shifted bands of cut 1188 bp fragment and the total number of counts in each lane (cut and uncut 1188 bp DNA fragments).

Site-Specific Binding Model. The equilibrium binding constant (K_{eq}) characterizes the affinity of a protein for its DNA binding site. For a reversible binding reaction

$$\text{protein} + \text{DNA} \leftrightarrow \text{protein}-\text{DNA} \quad (1)$$

the equilibrium binding constant is given by

$$K_{eq} = \frac{[\text{protein}-\text{DNA}]}{[\text{protein}][\text{DNA}]}. \quad (2)$$

The ratio ν of the concentration of EcoRI−DNA complexes to the total concentration of DNA molecules is

$$\nu = \frac{[\text{ADN}]_{tot} + [\text{protein}]_{tot} + 1/K_{eq}}{2[\text{ADN}]_{tot}} - \frac{\sqrt{([\text{ADN}]_{tot} + [\text{protein}]_{tot} + 1/K_{eq})^2 - 4[\text{ADN}]_{tot}[\text{protein}]_{tot}}}{2[\text{ADN}]_{tot}} \quad (3)$$

where $[\text{ADN}]_{tot}$ and $[\text{protein}]_{tot}$ are the total DNA and protein concentrations, respectively (*23*). The fit of experimental data with eq 3 also allows us to measure both the actively binding protein concentration and K_{eq}, as described previously (*23*).

RESULTS

For AFM imaging of the EcoRI−DNA complexes, the composition of the buffer should allow the protein binding to its DNA recognition site but not the DNA cleavage. In a previous study, Allison and co-workers (*5*) have used a mutant of EcoRI which binds to DNA with a 1000-fold greater binding affinity than the wild-type enzyme but with

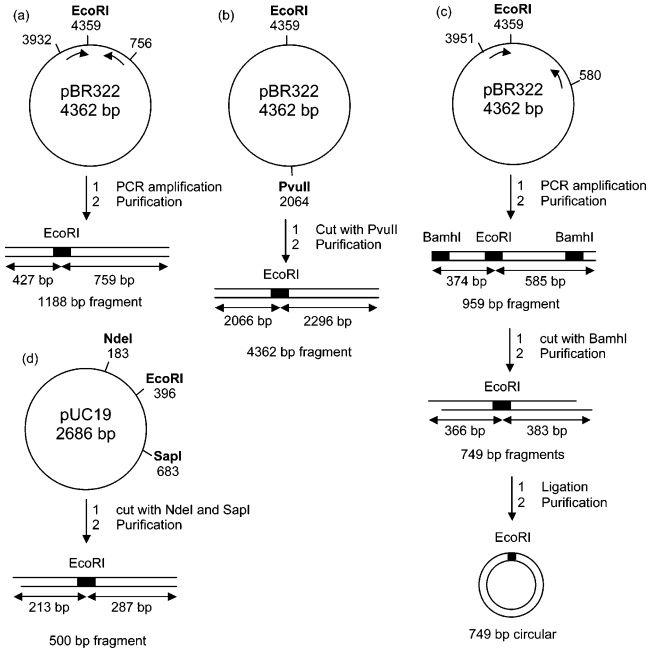

FIGURE 1: Scheme of DNA fragment constructions: (a) 1188 bp, (b) pBR322 linearization, (c) circular 750 bp, and (d) 500 bp. The localization of the EcoRI binding site is indicated for each fragment (see Materials and Methods for details).

cleavage rate constants reduced by a factor of 10^4. The use of the mutant then allowed the presence of Mg^{2+} in the binding buffer for observation of the EcoRI−DNA complexes on the mica surface. Another way is to use the wild-type enzyme in the absence of Mg^{2+} cations. Indeed, Mg^{2+} is not required for the binding of EcoRI to its DNA recognition site but is essential for the cleavage activity of the protein (*24*). Therefore, we have used Ca^{2+} instead of Mg^{2+} as divalent counterion to mediate adsorption of DNA and the EcoRI−DNA complex onto mica.

To measure ν, the ratio of the concentration of EcoRI−DNA complexes to the total concentration of DNA molecules versus EcoRI concentration by AFM, a 1188 bp DNA fragment was constructed. This fragment has only one EcoRI site located 427 bp from one end of the DNA (see Figure 1), which is approximately one-third of the DNA fragment length. Then it is easy to determine if the protein is site-specifically bound to the fragment by determining the protein position along the DNA molecule. Of course, the protein may be situated on the symmetrical but nonspecific position. However, this error can be neglected given the high lateral resolution of AFM. Indeed, the experimental error on the number of formed specific complexes due to the symmetrical nonspecific position is less than 4%. To estimate this error, one should consider that the protein position along the fragment is measured by AFM with an accuracy of ∼40 bp. Therefore, ∼30 positions can be distinguished along a 1188 bp fragment, and only two positions are considered to be specific instead of one.

AFM images of DNA molecules adsorbed on mica are represented in Figure 2 for different EcoRI concentrations. As observed, the presence of the enzyme at a specific position can be easily distinguished. It is worth noting that nonspecific binding to DNA represents less than 5% of the total EcoRI−DNA complexes. When the enzyme concentration is increased, ν increases, as expected. However, we should note

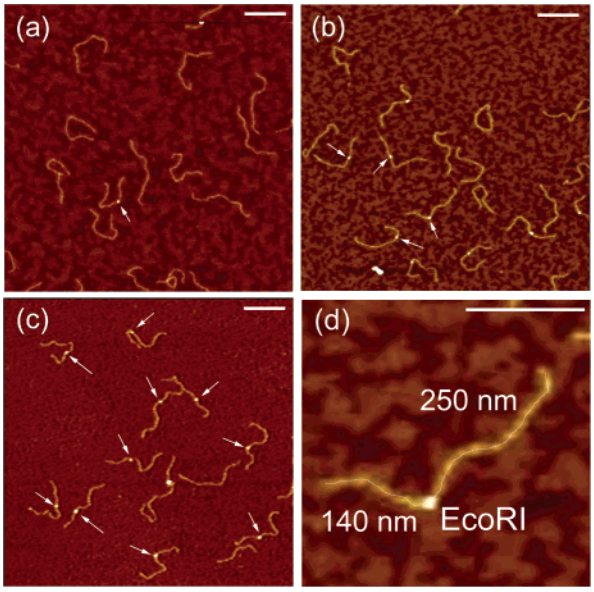

FIGURE 2: AFM images of binding of EcoRI on the 1188 bp DNA fragment which contained a single EcoRI-specific binding site located 429 bp from one end of the DNA fragment [20 mM Tris (pH 7.5), 20 mM NaCl, and 10 mM $CaCl_2$]. The DNA concentration was fixed at 0.2 nM, and gradually increasing EcoRI concentrations were used: (a) 10, (b) 60, and (c) 125 nM (scale bar of 200 nm). EcoRI proteins are clearly distinguished on the DNA thread (see arrows). As the protein concentration is increased, more and more specific complexes are observed on the mica surface. (d) Close-up of an EcoRI protein bound to a DNA molecule (scale bar of 150 nm). The distances from the bound protein to the two ends are 140 and 250 nm, respectively. This indicates that the protein is located on its specific site.

that the EcoRI concentration required to obtain more than 50% of the complexes is rather high (0.5 nM DNA molecules/10 nM EcoRI). It clearly indicates that dissociation takes place during the adsorption process.

The ratio ν measured in solution by gel shift assays versus EcoRI concentration is shown in Figure 3a for various EcoRI concentrations at low and high ionic strengths. The gel shift assay study was performed to determine the molar concentration of actively binding EcoRI. In addition, the binding constant of the specific EcoRI−DNA complex was measured at low and high ionic strengths (2.5×10^{11} and 1.7×10^{7} M^{-1} at low and high ionic strengths, respectively). These results, which are in agreement with those reported previously (*21*, *23*, *25*), enable the comparison between AFM and gel shift assay measurements by using the same protein solution.

Figure 3b represents ν versus the EcoRI concentration obtained by AFM on the mica surface at low and high ionic strengths. The point is that the EcoRI concentration required to image a significant percentage of adsorbed specific complexes is 2 orders of magnitude higher than DNA concentration. This is particularly pronounced at low ionic strengths for which saturation of the DNA-specific sites is reached at 20 nM EcoRI and 10 nM DNA molecules for gel shift assays and 125 nM EcoRI and 0.2 nM DNA molecules for AFM measurements. Consequently, the measured binding constants on the surface were lower than those in solution (1×10^{7} and 2.6×10^{6} M^{-1} at low and high ionic strengths, respectively). The relatively small difference between AFM and EMSA experiments at high ionic strengths can be explained by the presence of $CaCl_2$ in the deposition buffer for adsorption of DNA. Indeed, divalent cations can lower the equilibrium binding constant (*26*). Therefore, we suggest that AFM and EMSA measurements are quite similar at high ionic strengths. With regard to the low ionic strength measurements, the presence of 10 mM $CaCl_2$ in the deposition buffer at low ionic strengths cannot explain the observed large discrepancy (the binding constant on the surface is ~4 orders of magnitude lower). Consequently, only the surface effect can account for the biased value of the binding constant at low ionic strengths.

The influence of the DNA length on ν, the ratio of the concentration of EcoRI−DNA complexes to the total concentration of adsorbed DNA molecules, was also studied by AFM. In these experiments, the EcoRI concentration was significantly higher than the DNA concentration so that the concentration of free DNA molecules in solution prior to adsorption could be neglected. The ratio ν was measured on the surface at low ionic strength for different fragment lengths (500, 1188, and 4362 bp) (see Figure 4). It appears that the degree of dissociation of the specific complex increases when

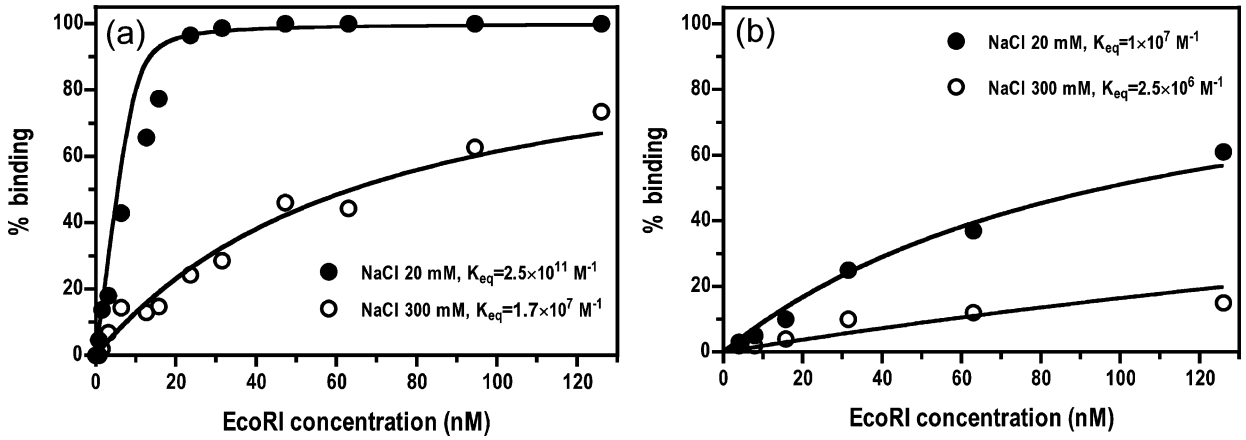

FIGURE 3: Plot of ν, the ratio of the concentration of EcoRI−DNA complexes to the total concentration of DNA molecules, vs EcoRI concentration at low [20 mM Tris (pH 7.5) and 20 mM NaCl] and high ionic strengths [20 mM Tris (pH 7.5) and 300 mM NaCl] determined by gel shift assays at a DNA concentration of 10 nM (a) and by AFM at a DNA concentration of 0.2 nM (b). It is worth noting that the EcoRI−DNA binding constants measured by AFM are smaller than those measured by EMSA. This is particularly pronounced at low ionic strengths, which indicates that the binding affinity of a protein for its specific DNA site is dramatically reduced upon adsorption of DNA on mica.

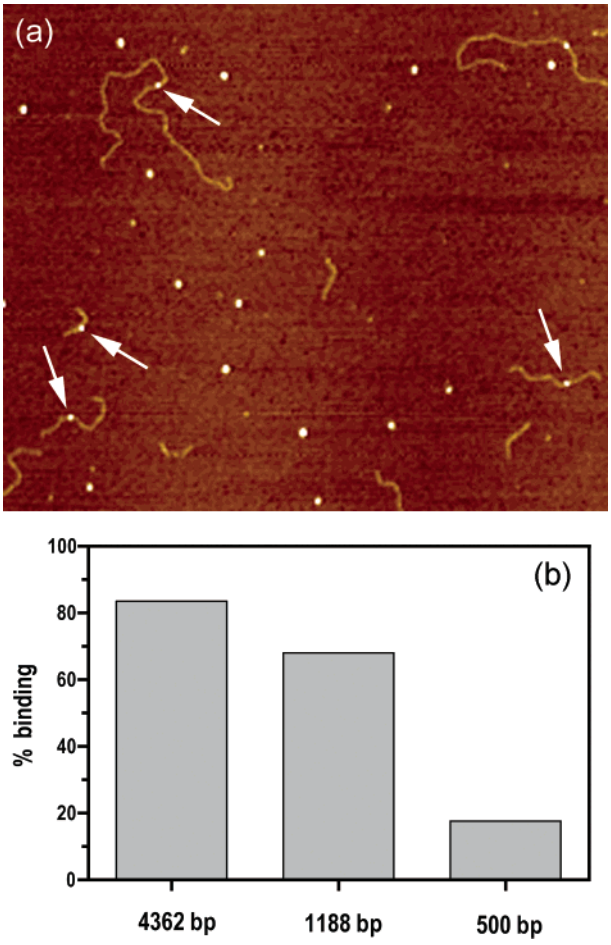

FIGURE 4: AFM measurements of ν for three different DNA fragment lengths (4362, 1188, and 500 bp). The deposition buffer contained the three DNA fragments with an EcoRI concentration in large excess so that all the DNA fragments have formed a complex in solution prior to deposition [20 mM Tris (pH 7.5), 20 mM NaCl, and 10 mM $CaCl_2$; 0.2 nM 4362 bp DNA, 0.2 nM 1188 bp DNA, and 0.3 nM 500 bp DNA; and 30 nM EcoRI]. (a) AFM image of the EcoRI−DNA complexes adsorbed on the surface. Specific binding to the DNA fragment is easily observed (see arrows). We can also note that only one-third of the 500 bp fragments has formed a complex in this image. (b) Diagram of ν values for the three DNA fragments.

the DNA fragment length decreases, which is the opposite of what happens in solution. Indeed, in solution at low and moderate ionic strengths, the dissociation of the specific complex is favored by the protein binding to nonspecific DNA sites. Therefore, the dissociation probability increases with DNA fragment length (*21*). On the mica surface, the influence of DNA length on the dissociation probability seems to be similar to that observed in solution at high ionic strengths (>150 mM) for which the dissociation probability of the shorter fragments is more important. Another hypothesis could be that the proximity of a DNA fragment end to the specific site favors the protein dissociation on the mica surface even though it has been demonstrated that DNA ends have no effect on complex dissociation in solution (*21*). To test that hypothesis, we prepared a solution which contained a mix of a 500 bp linear fragment and a 750 bp circularized fragment with EcoRI in large excess. The same ratio binding ratio was obtained for both DNA fragments. This indicates that DNA ends have no significant effect on dissociation of the complex.

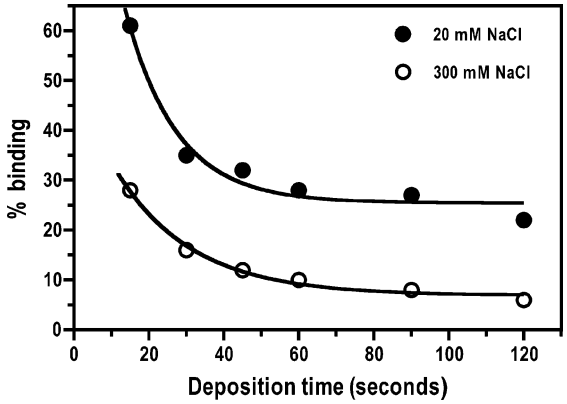

FIGURE 5: Plot of ν for adsorbed DNA molecules vs the deposition time at low [20 mM Tris (pH 7.5), 20 mM NaCl, and 10 mM $CaCl_2$] and high ionic strengths [20 mM Tris (pH 7.5), 300 mM NaCl, and 100 mM $CaCl_2$]. The DNA concentration was 0.2 nM and the EcoRI concentrations 60 nM. We observe a slow dissociation ($\tau \approx 60$ s) that is not expected at high ionic strengths in solution ($\tau \ll 15$ s when $I > 200$ mM).

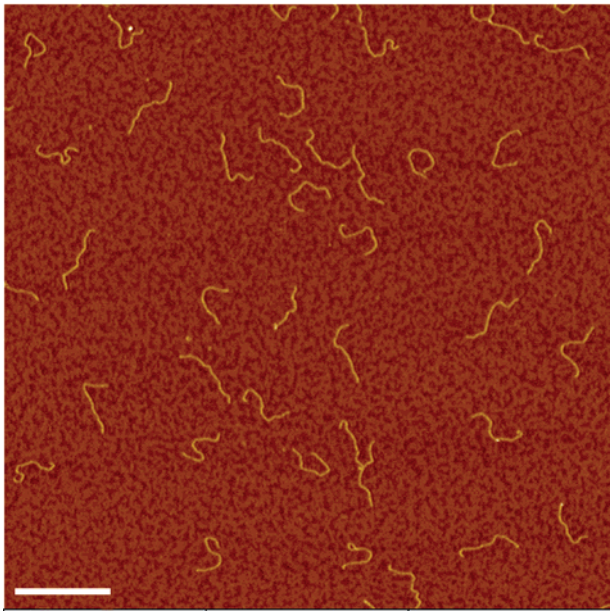

FIGURE 6: AFM image obtained after deposition of the purified specific EcoRI−DNA complex [20 mM Tris (pH 7.5), 20 mM NaCl, and 10 mM $CaCl_2$]. This indicates that EcoRI is not attracted on the mica surface as it dissociates from DNA upon adsorption (scale bar of 250 nm).

We have also studied the dissociation of the complexes once adsorbed on the surface versus the deposition time both at low and high ionic strengths. After a short DNA deposition time (15 s), the drop is diluted 10 times to stop the adsorption of additional DNA molecules to the mica. Figure 5 represents the slow dissociation of the complexes on the surface versus deposition time. The kinetics of this dissociation seems to be weakly dependent on the ionic strength of the solution. The time required for half the complexes to dissociate is ~60 s. Besides, it is worth noting that control experiments showed that DNA molecules adsorbed on the surface prior to addition of EcoRI are hardly accessible to the protein under the conditions studied here (data not shown). Therefore, the association of a protein to a free adsorbed fragment can be neglected.

One hypothesis for the origin of the dissociation of the complex once adsorbed on the surface could be the high affinity of the protein for the surface. However, we rarely observed a protein adsorbed on the surface near the specific site, which could have indicated the affinity of the protein for mica. In addition, only few free proteins were adsorbed on the surface even though the protein concentration was significantly higher than the DNA concentration. To make sure that released proteins were not attracted on the mica surface upon dissociation, the EcoRI−DNA complexes were formed in solution and purified by size exclusion chromatography to remove the unbound proteins. The complex was then eluted in less than 2 min, a period sufficiently short to prevent its dissociation at low ionic strengths [20 mM NaCl and 20 mM Tris (pH 7.5)] (*21*). The purified complex was immediately deposited onto mica and imaged by AFM (Figure 6). We controlled by gel electrophoresis the fact that the EcoRI−DNA complex did not dissociate during size exclusion chromatography (data not shown). The AFM images show that there was no protein on the DNA molecules or on the surface. This means that all the complexes were dissociated and the proteins were released from the surface into the solution.

DISCUSSION

Very few quantitative AFM studies of protein−protein interactions (*27*) or protein−DNA interactions (*3*, *28*−*30*) have been undertaken so far. In addition, the presence of the surface as an interacting body has been neglected. In a recent work performed by Yang and co-workers on the MutS−DNA complex (*3*), the primary assumption for measuring the binding constants of the complex by AFM was that the populations of bound and free DNA on the surface are the same as those in solution, i.e., that deposition on the surface does not alter the populations. This assumption is not valid for the EcoRI−DNA complexes since the value of the ratio of the concentration of EcoRI−DNA complexes to the total concentration of DNA molecules, ν, in solution is larger than the value measured by AFM. One explanation could be that the complex does not adsorb as strongly on the surface as a free DNA molecule does. However, it seems highly unlikely that the presence of a small protein on a long DNA fragment could change significantly the binding strength on the mica surface. More likely is the possibility that the effect of the surface biases the AFM measurements. The analysis of our experimental results provides a great piece of information about the surface influence.

Thermodynamic Equilibrium in the Vicinity of the Surface. The first point is that at low ionic strengths the binding constant of the complex on the surface is significantly lower than in solution, whereas at high ionic strengths, the binding constants are quite similar in solution and on the surface. It seems like the ionic strength on the surface is higher than that in bulk. In addition, the ionic strength near the surface appears to be weakly sensitive to the ionic strength of the solution. To understand this, one has to consider the mica surface as a highly negatively charged surface. The monovalent counterion concentration increases dramatically at the surface to neutralize it. Using the nonlinear Poisson−Boltzmann equation, the counterion concentration decay is (*31*)

$$n(d) = \frac{2\pi(\sigma/e)^2 l_B}{[1 + d/(2e/4\pi\sigma l_B z)]^2} + n_b \qquad (4)$$

where d is the distance from the surface, n_b the bulk concentration of the counterion species, e the electron charge, σ the surface charge density, l_B the Bjerrum length, and z the counterion valence.

For the mica surface, the monovalent salt concentration 1 nm from the mica surface is greater than 300 mM whatever the bulk monovalent salt concentration (*31*). The mica surface charge density in solution is equal to 2 e^-/nm^2 (*32*). It results from the release of potassium ions on the mica surface, without taking into account the neutralization by the adsorbed cations. Indeed, under typical solution conditions, most of the negative lattice sites are neutralized with condensed cations (Na^+, Mg^{2+}, etc.) (*32*, *33*). As it was reported that DNA counterions should be located less than l_B ($\cong$0.7 nm) from the surface to allow DNA adsorption (*12*, *14*), the adsorbed DNA molecules are then partly embedded in the counterion cloud in which the Na^+ concentration is weakly dependent on the buffer composition. As a consequence, the thermodynamic parameters governing EcoRI−DNA interactions are not the same on the mica surface and in solution at low bulk ionic strengths.

Further support for this observation is the effect of the DNA length on ν for adsorbed molecules at low bulk ionic strengths. It appears that the dissociation of the complexes on the mica surface is more complete for the shorter DNA fragments. Consequently, the dissociation of the protein−DNA complex due to the adsorption on the mica surface is not mediated by the nonspecific protein binding to DNA. This is generally observed in solution at high ionic strengths (*21*).

As the ionic strength felt by the adsorbed complexes is larger than in bulk, it should cause a shift in the thermodynamic equilibrium similar to what is observed in solution when the ionic strength is increased. This equilibrium shift takes place when the DNA molecules are interacting with the surface but are not yet fully adsorbed on the surface. The measured values of the equilibrium constants are therefore influenced by this intermediate state. It is also worth noting that, upon adsorption, the binding of EcoRI to DNA prevents some divalent counterions from participating in the DNA adsorption via counterion correlations. This energy penalty is an additional factor which may facilitate dissociation of EcoRI to increase the energy benefit of DNA adsorption.

Dissociation of the Complexes Once Adsorbed on the Surface. Once adsorbed, the protein−DNA complexes undergo an irreversible dissociation. Indeed, the specific binding of the free protein to adsorbed DNA was not significant under the conditions studied here. As previously reported for drug−DNA interactions (*15*, *16*), strong surface binding on mica could affect DNA accessibility. As EcoRI is a larger ligand than drugs, the accessibility of DNA to EcoRI should be even more diminished, which could preclude EcoRI−DNA association on the surface. However, what is more surprising is the slowness of the dissociation (half-time $\tau \approx 60$ s) that is not expected at high ionic strengths in solution [>200 mM NaCl, $\tau \ll 15$ s (*21*)]. One explanation could be that the surface friction due to the mica

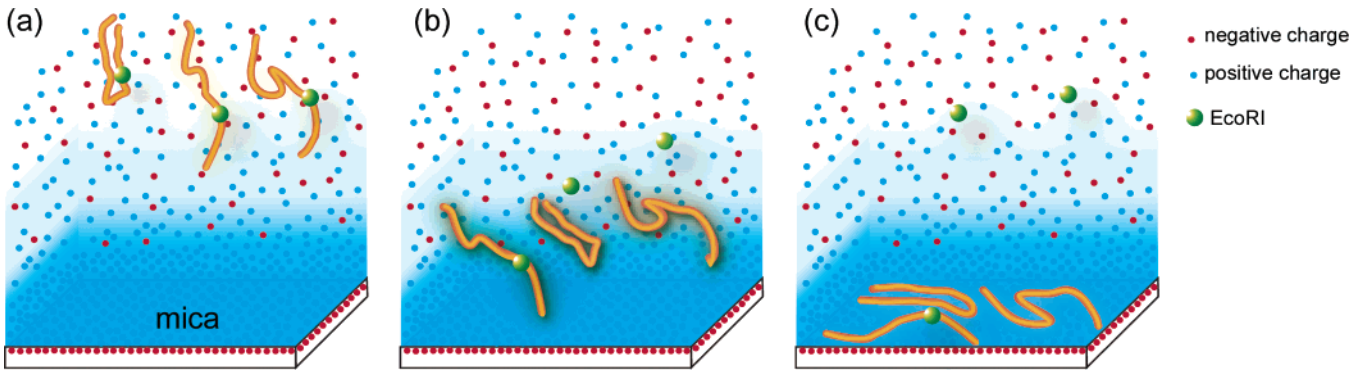

FIGURE 7: Scheme of the two-step adsorption process. (a) EcoRI−DNA complexes are formed in solution. As the complexes approach the highly charged mica surface, the ionic strength increases. (b) It results in a dissociation of some complexes until the molecules are fully adsorbed. Dissociated proteins are released in the solution and not on the surface because of their low affinity for the mica surface. (c) Once fully adsorbed on the surface (with a two-dimensional conformation), the remaining EcoRI−DNA complexes undergo a slow dissociation.

and DNA counterions hinders the complex dissociation. Indeed, the environment near the surface is crowded with counterions, which slows DNA diffusion on mica (*15*). Furthermore, it is generally accepted that environments crowded with PEG molecules or sucrose (*34*) increase the dissociation time by changing the water activity. As the crowd of counterions on the surface could also considerably lower the water activity, this might be another explanation. With regard to the slow dissociation of the adsorbed complexes, we have noted that its kinetics seems to be weakly dependent on the bulk ionic strength. This is not surprising since, whatever the bulk ionic strength, the surface ionic strength remains very high.

Mechanism of Adsorption of DNA−Protein Complex and Practical Interests. By considering the analysis of this work, we propose a two-step mechanism for the adsorption of EcoRI−DNA complexes on a mica surface (Figure 7).

First, the EcoRI−DNA complex in solution approaches the surface due to the attraction between the DNA molecule and the mica surface mediated by multivalent counterions. This is a short-range attraction, and only some parts of the DNA molecule are interacting with the surface before the complex is fully adsorbed. Indeed, the DNA molecule adopts a three-dimensional conformation in solution, and some rearrangements are necessary for the molecule to adopt a two-dimensional conformation on the surface. During this step, the ionic conditions in the vicinity of the surface cause a shift of the equilibrium toward the equilibrium that prevails at high ionic strengths. Therefore, many EcoRI−DNA complexes dissociate since the equilibrium binding constant of the complex decreases with the increase in ionic strength. The point is that AFM measurements could be more relevant if they were performed at high ionic strengths ($I > 100$ mM), where the DNA ionic environments on the surface and in solution are quite similar. Furthermore, working at high ionic strengths is important in approaching the physiological conditions. The equilibrium shift must have been a problem for AFM users, who generally used a low-ionic strength solution to adsorb protein−DNA complexes on mica. Indeed, as indicated by our results and those reported previously by Lysetska et al. (*4*), the protein concentration required to observe DNA−protein complexes on the surface can be significantly higher than the concentration required to form the complexes in solution at low ionic strengths. The drawback is that the protein surface coverage due to nonspecific adsorption at low ionic strengths can be quite important if a high protein concentration is used, which could affect the imaging conditions (*35*).

Second, the complexes become fully adsorbed on the surface. Then a slow dissociation of the complexes on the surface takes place with a half-life of ∼60 s. This slow dissociation is likely due to the presence of the condensed counterion layer on the mica surface, which can lower the water activity and induce a strong surface friction. These effects slow the dissociation whatever the NaCl concentration. To our knowledge, the dissociation of the protein−DNA complexes on mica has never been depicted. A direct practical interest of this observation is that the AFM study of the complex is time-limited. Indeed, an EcoRI−DNA complex adsorbed on the surface can hardly be imaged by AFM in liquid for more than 1 or 2 min. Thus, successive AFM images of the complex must be taken within a few minutes, which may be difficult but possible. It means that the EcoRI−DNA complexes should be injected into the AFM liquid cell while the AFM tip scans the mica surface and all the AFM parameters are adjusted for proper imaging. This is a desirable piece of knowledge for those interested in using AFM to study protein−DNA interactions in liquid. The results presented in this paper can surely be extended to many other proteins which interact specifically with DNA.

REFERENCES

1. van Gent, D. C., Hoeijmakers, J. H., and Kanaar, R. (2001) Chromosomal stability and the DNA double-stranded break connection, *Nat. Rev. Genet. 2*, 196−206.
2. Shin, D. S., Chahwan, C., Huffman, J. L., and Tainer, J. A. (2004) Structure and function of the double-strand break repair machinery, *DNA Repair 3*, 863−873.
3. Yang, Y., Sass, L. E., Du, C., Hsieh, P., and Erie, D. A. (2005) Determination of protein-DNA binding constants and specificities from statistical analyses of single molecules: MutS-DNA interactions, *Nucleic Acids Res. 33*, 4322−4334.
4. Lysetska, M., Zettl, H., Oka, I., Lipps, G., Krauss, G., and Krausch, G. (2005) Site-specific binding of the 9.5 kilodalton DNA-binding protein ORF80 visualized by atomic force microscopy, *Biomacromolecules 6*, 1252−1257.
5. Allison, D. P., Kerper, P. S., Doktycz, M. J., Spain, J. A., Modrich, P., Larimer, F. W., Thundat, T., and Warmack, R. J. (1996) Direct atomic force microscope imaging of EcoRI endonuclease site specifically bound to plasmid DNA molecules, *Proc. Natl. Acad. Sci. U.S.A. 93*, 8826−8829.
6. Abdelhady, H. G., Allen, S., Davies, M. C., Roberts, C. J., Tendler, S. J. B., and Williams, P. M. (2003) Direct real-time molecular

scale visualisation of the degradation of condensed DNA complexes exposed to DNase I, *Nucleic Acids Res. 31*, 4001−4005.

7. Bezanilla, M., Drake, B., Nudler, E., Kashlev, M., Hansma, P. K., and Hansma, H. G. (1994) Motion and enzymatic degradation of DNA in the atomic force microscope, *Biophys. J. 67*, 2454−2459.
8. Chen, L., Haushalter, K. A., Lieber, C. M., and Verdine, G. L. (2002) Direct visualization of a DNA glycosylase searching for damage, *Chem. Biol. 9*, 345−350.
9. Tessmer, I., Moore, T., Lloyd, R. G., Wilson, A., Erie, D. A., Allen, S., and Tendler, S. J. (2005) AFM studies on the role of the protein RdgC in bacterial DNA recombination, *J. Mol. Biol. 350*, 254−262.
10. Ristic, D., Modesti, M., Kanaar, R., and Wyman, C. (2003) Rad52 and Ku bind to different DNA structures produced early in double-strand break repair, *Nucleic Acids Res. 31*, 5229−5237.
11. Moreno-Herrero, F., Perez, M., Baro, A. M., and Avila, J. (2004) Characterization by atomic force microscopy of Alzheimer paired helical filaments under physiological conditions, *Biophys. J. 86*, 517−525.
12. Pastré, D., Piétrement, O., Fusil, S., Landousy, F., Jeusset, J., David, M. O., Hamon, L., Le Cam, E., and Zozime, A. (2003) Adsorption of DNA to mica mediated by divalent counterions: A theoretical and experimental study, *Biophys. J. 85*, 2507−2518.
13. Rivetti, C., Guthold, M., and Bustamante, C. (1996) Scanning force microscopy of DNA deposited onto mica: Equilibration versus kinetic trapping studied by statistical polymer chain analysis, *J. Mol. Biol. 264*, 919−932.
14. Pastré, D., Hamon, L., Landousy, F., Sorel, I., David, M. O., Zozime, A., Le Cam, E., and Piétrement, O. (2006) Anionic Polyelectrolyte Adsorption on Mica Mediated by Multivalent Cations: A Solution to DNA Imaging by Atomic Force Microscopy under High Ionic Strengths, *Langmuir 22*, 6651−6660.
15. Pastré, D., Piétrement, O., Zozime, A., and Le Cam, E. (2005) Study of the DNA/ethidium bromide interactions on mica surface by atomic force microscope: Influence of the surface friction, *Biopolymers 77*, 53−62.
16. Piétrement, O., Pastré, D., Landousy, F., David, M. O., Fusil, S., Hamon, L., Zozime, A., and Le Cam, E. (2005) Studying the effect of a charged surface on the interaction of bleomycin with DNA using an atomic force microscope, *Eur. Biophys. J. 34*, 200−207.
17. Terry, B. J., Jack, W. E., Rubin, R. A., and Modrich, P. (1983) Thermodynamic parameters governing interaction of EcoRI endonuclease with specific and nonspecific DNA sequences, *J. Biol. Chem. 258*, 9820−9825.
18. McClarin, J. A., Frederick, C. A., Wang, B. C., Greene, P., Boyer, H. W., Grable, J., and Rosenberg, J. M. (1986) Structure of the DNA-EcoRI endonuclease recognition complex at 3 Å resolution, *Science 234*, 1526−1541.
19. Wright, D. J., Jack, W. E., and Modrich, P. (1999) The kinetic mechanism of EcoRI endonuclease, *J. Biol. Chem. 274*, 31896−31902.
20. Rouzina, I., and Bloomfield, V. A. (1996) Competitive electrostatic binding of charged ligands to polyelectrolytes: Planar and cylindrical geometries, *J. Phys. Chem. 100*, 4292−4304.
21. Jack, W. E., Terry, B. J., and Modrich, P. (1982) Involvement of outside DNA sequences in the major kinetic path by which EcoRI endonuclease locates and leaves its recognition sequence, *Proc. Natl. Acad. Sci. U.S.A. 79*, 4010−4014.
22. Revet, B., and Fourcade, A. (1998) Short unligated sticky ends enable the observation of circularised DNA by atomic force and electron microscopies, *Nucleic Acids Res. 26*, 2092−2097.
23. Rippe, K. (1997) Analysis of protein-DNA binding at equilibrium, *Futura 12*, 20−26.
24. Modrich, P. (1979) Structures and mechanisms of DNA restriction and modification enzymes, *Q. Rev. Biophys. 12*, 315−369.
25. Wright, D. J., King, K., and Modrich, P. (1989) The negative charge of Glu-111 is required to activate the cleavage center of EcoRI endonuclease, *J. Biol. Chem. 264*, 11816−11821.
26. King, K., Benkovic, S. J., and Modrich, P. (1989) Glu-111 is required for activation of the DNA cleavage center of EcoRI endonuclease, *J. Biol. Chem. 264*, 11807−11815.
27. Ratcliff, G. C., and Erie, D. A. (2001) A novel single-molecule study to determine protein−protein association constants, *J. Am. Chem. Soc. 123*, 5632−5635.
28. Kasas, S., Thomson, N. H., Smith, B. L., Hansma, H. G., Zhu, X., Guthold, M., Bustamante, C., Kool, E. T., Kashlev, M., and Hansma, P. K. (1997) *Escherichia coli* RNA polymerase activity observed using atomic force microscopy, *Biochemistry 36*, 461−468.
29. Solis, F. J., Bash, R., Yodh, J., Lindsay, S. M., and Lohr, D. (2004) A statistical thermodynamic model applied to experimental AFM population and location data is able to quantify DNA-histone binding strength and internucleosomal interaction differences between acetylated and unacetylated nucleosomal arrays, *Biophys. J. 87*, 3372−3387.
30. Yaneva, M., Kowalewski, T., and Lieber, M. R. (1997) Interaction of DNA-dependent protein kinase with DNA and with Ku: Biochemical and atomic-force microscopy studies, *EMBO J. 16*, 5098−5112.
31. Rouzina, I., and Bloomfield, V. A. (1996) Influence of ligand spatial organization on competitive electrostatic binding to DNA, *J. Phys. Chem. 100*, 4305−4313.
32. Pashley, R. M., and Israelachvili, J. N. (1984) DLVO and hybridation forces between mica surfaces in Mg^{2+}, Ca^{2+}, Sr^{2+} and Ba^{2+} chloride solutions, *J. Colloid Interface Sci. 97*, 446−455.
33. Pashley, R. M., and Quirk, J. P. (1984) The effect of cation valency on DLVO and hydration forces between macroscopic sheets of muscovite mica in relation to clay swelling, *Colloids Surf. 9*, 1−17.
34. Sidorova, N. Y., and Rau, D. C. (2001) Linkage of EcoRI dissociation from its specific DNA recognition site to water activity, salt concentration, and pH: Separating their roles in specific and non-specific binding, *J. Mol. Biol. 310*, 801−816.
35. Czajkowsky, D. M., and Shao, Z. (2003) Inhibition of protein adsorption to muscovite mica by monovalent cations, *J. Microsc. 211*, 1−7.

BI060293U